Nuclear Magnetic Resonance Line Shapes Resulting from the Combined Effects of Nuclear Quadrupole and Anisotropic Shift Interactions*

W. H. JONES, JR.,† T. P. GRAHAM, AND R. G. BARNES
Institute for Atomic Research and Department of Physics, Iowa State University, Ames, Iowa
(Received 12 September 1962; revised manuscript received 9 August 1963)

The effects on the nuclear magnetic resonance line shape of a polycrystalline sample resulting from combined axially symmetric electric quadrupole and anisotropic shift interactions have been calculated through the second order. The line shape of the central transition of the resonance has been shown to change smoothly from that characteristic of quadrupole effects (inverse field dependence) to that characteristic of anisotropic shift effects (direct field dependence) as the magnetic field strength is increased. Methods are given for determining the magnetic shift parameters—both isotropic and anisotropic (axial)—and the electric quadrupole coupling from line shape and shift measurements. An illustration of these methods is given, based on experimental measurements of the Al^{27} spectrum in polycrystalline $PrAl_2$.

INTRODUCTION

A NUCLEAR quadrupole interaction may occur simultaneously in conjunction with an anisotropic magnetic shift in a variety of solids. The noncubic pure metals, in particular the hexagonal close-packed ones, afford a considerable number of examples, some which have already been studied. Among the latter may be listed Sc,[1] In,[2] Tc,[3] and the list of possibilities must include Ti, Zr, Hf, La, and Lu and perhaps others. Nuclear magnetic resonances (NMR) in intermetallic compounds may also be expected to exhibit these combined effects. The cubic Laves phase compounds of the $MgCu_2$ type have provided a number of examples, principally involving the Al^{27} nucleus.[4,5] Transition metal borides[6] and beryllides, as well as other hexagonal and tetragonal intermetallics may also be included in this category. Finally, the nuclear magnetic resonance of the halogen nuclei in the paramagnetic chlorides, bromides, and iodides of transition metals will, in general, reflect the presence of both types of interaction.[7]

In the following sections the theory for these combined effects is considered in some detail. The separate cases of quadrupolar and anisotropic shift effects have been discussed individually at length, both in the journal literature and in reviews, and only brief recapitulations of these will be presented here, in order to point up the differences and similarities that exist between them and the case in which the two effects are interwoven. Averaged line-shape patterns appropriate to polycrystalline (powder) samples are given for various relative strengths of the two effects, and the behavior of various experimentally observed quantities (linewidths, shifts) are calculated as functions of resonance frequency for some combinations of values of the quadrupole and shift parameters typical of those already observed. These calculations also include in an empirical manner the effects of a frequency-independent linewidth (nuclear dipolar, etc.) on the expected experimental behavior. Finally, a number of experimental cases are considered which illustrate the method of analysis to determine the various interaction parameters.

THEORY

Quadrupolar Effects Only

The effects of electric quadrupole interactions on the Zeeman energy of the nuclear magnetic moment were first discussed by Pound,[8] who gave formulas for the levels and transitions to be expected in the case of single-crystal specimens. Because the electric field gradient tensor is an intrinsic property of the sample, these levels and the transitions between them are dependent upon the orientation of the crystal in the external magnetic field. For polycrystalline specimens, such as are required in the case of metallic conductors, these results must be averaged over all possible orientations of the crystallites. The review article of Cohen and Reif,[9] for example, explains how this averaging is carried out.

In the absence of anisotropic magnetic shift complications, and for the case of an axially symmetric field gradient tensor, the expression correct to second order for the transition frequencies appropriate to a nucleus of spin I in a single crystal specimen is

$$\nu(m\leftrightarrow m-1)$$
$$=\nu_0+\tfrac{1}{2}\nu_Q(3\mu^2-1)(m-\tfrac{1}{2})+(\nu_Q^2/32\nu_0)(1-\mu^2)\times\{[102m(m-1)-18I(I+1)+39]\mu^2-[6m(m-1)-2I(I+1)+3]\}. \quad (1)$$

* Contribution No. 1202. Work was performed in the Ames Laboratory of the U. S. Atomic Energy Commission.
† Present address: Battelle Memorial Institute, Columbus, Ohio.
[1] S. L. Segel and R. G. Barnes, Bull. Am. Phys. Soc. **7**, 537 (1962).
[2] D. R. Torgenson and R. G. Barnes, Phys. Rev. Letters **9**, 255 (1962).
[3] W. H. Jones, Jr. and F. J. Milford, Phys. Rev. **125**, 1259 (1962).
[4] V. Jaccarino, B. T. Matthias, M. Peter, H. Suhl, and J. H. Wernick, Phys. Rev. Letters **5**, 251 (1960); V. Jaccarino, J. Appl. Phys. **32**, 102S (1961).
[5] R. G. Barnes, W. H. Jones, Jr., and T. P. Graham, Phys. Rev. Letters **6**, 221 (1961).
[6] A. H. Silver and T. Kushida, Bull. Am. Phys. Soc. **7**, 226 (1962).
[7] R. G. Barnes and S. L. Segel, J. Chem. Phys. **37**, 1895 (1962).
[8] R. V. Pound, Phys. Rev. **79**, 685 (1950).
[9] M. H. Cohen and F. Reif, in *Solid State Physics*, edited by F. Seitz and D. Turnbull (Academic Press Inc., New York, 1957), Vol. 5, p. 311.

Here, $\nu_Q=3e^2qQ/2I(2I-1)h$ is a convenient measure of the strength of the quadrupole interaction, and $\mu=\cos\theta$, where θ is the angle between the z axis of the principal axis system of the field gradient tensor and the external magnetic field. In this equation, the factor ν_0 is the pure Zeeman transition frequency (Larmor frequency) in the absence of electric quadrupole interaction. It reflects the fact that the pure Zeeman levels are equally spaced. The term independent of ν_0 arises from first-order perturbation theory and affects the so-called "satellite" transitions only. That is, the central, or $\frac{1}{2}\leftrightarrow-\frac{1}{2}$, transition is unshifted in first order, and satellite resonances appear, placed symmetrically with respect to it. In second-order theory, the terms in ν_Q^2/ν_0 are obtained, all of the transitions being affected, although the satellites are shifted equally in pairs.

In the case of a polycrystalline sample, the expressions corresponding to (1) are those that give the frequencies at which the intensity maxima in the averaged resonance line shape occur. As shown by Cohen and Reif,[9] for example, intensity maxima for the satellites will always occur for $\theta=90°$ ($\mu=0$), so that for the polycrystalline sample, satellite resonance peaks will appear at

$$\nu(m\rightarrow m-1)=\nu_0-\tfrac{1}{4}\nu_Q(2m-1)-(\nu_Q^2/16\nu_0)\times[3m(m-1)-I(I+1)+\tfrac{3}{2}]. \quad (2)$$
$$m\neq\tfrac{1}{2}$$

In addition, other intensity maxima will arise at other values of θ or μ when the second-order frequency dependence of the satellites is taken into account. These additional satellites are important only in the case of large quadrupole coupling and large spin.[2]

It is clear that although the satellites are asymmetrically placed with respect to the center point of the entire resonance pattern because of the second-order contribution, the spacing between corresponding opposite satellites always has a constant value. Thus, for example,

$$\nu(-m+1\leftrightarrow-m)-\nu(m\leftrightarrow m-1)=\tfrac{1}{2}\nu_Q(2m-1). \quad (3)$$

Finally, because of the particular orientation dependence which the central transition acquires in second order, the averaged expression for it possesses two maxima.[9] These correspond to $\mu=0$ and $\mu^2=5/9$, and the frequencies at which these maxima occur are given by

$$\nu^{\mathrm{I}}(\tfrac{1}{2}\leftrightarrow-\tfrac{1}{2})=\nu_0+(\nu_Q^2/16\nu_0)[I(I+1)-\tfrac{3}{4}] \quad (4)$$

$$\nu^{\mathrm{II}}(\tfrac{1}{2}\leftrightarrow-\tfrac{1}{2})=\nu_0-(\nu_Q^2/9\nu_0)[I(I+1)-\tfrac{3}{4}]. \quad (5)$$

In addition to these maxima, a small discontinuity or "step" appears at $\nu=\nu_0$. When dipolar broadening effects are taken into account this step is very much smoothed over so that it is only rarely discernable experimentally. The spacing between the two peaks (4) and (5)—in effect, the "width" or splitting of the central transition—is inversely proportional to the Zeeman frequency ν_0,

$$\Delta\nu=\nu^{\mathrm{I}}-\nu^{\mathrm{II}}=(25\nu_Q^2/144\nu_0)[I(I+1)-\tfrac{3}{4}]. \quad (6)$$

In a paramagnetic substance the pure Zeeman resonance frequency ν_0 will differ from its value in a diamagnetic (reference) environment by an amount which is usually expressed as the paramagnetic shift (Knight shift in the case of a metal),

$$K=(\nu_0-\nu_R)/\nu_R \quad (7)$$

for measurements made at constant magnetic field strength, and by

$$K=(H_R-H_0)/H_0 \quad (8)$$

for measurements made at constant resonance frequency. For the case of resonances in polycrystalline samples in which electric quadrupole effects are also present, so that (2), (4), and (5) describe the location of the resonance peaks, this shift may be measured by locating the true center of the resonance pattern using (4) and (5), and determining the shift of this point from the diamagnetic standard resonance. Since the resonance pattern will usually be observed at a number of frequencies to verify the quadrupolar effects, an alternative and convenient means of measuring the shift is to measure the shift of the midpoint of the two peaks of the central transition. Since these two peaks coalesce into one at infinite field strength (frequency), this "average" shift will extrapolate to the true shift at infinite field. In fact, this average shift is inversely proportional to the square of the resonance frequency:

$$K_{AV}=\frac{\frac{1}{2}(\nu^{\mathrm{I}}+\nu^{\mathrm{II}})-\nu_R}{\nu_R}=\frac{\nu_0-\nu_R}{\nu_R}-\frac{7}{288}\frac{\nu_Q^2}{\nu_R^2}[I(I+1)-\tfrac{3}{4}]. \quad (9)$$

To summarize, if electric quadrupole effects only are present, the nmr of a nucleus in a metallic conductor or paramagnetic solid will be characterized by

(a) A set of $2I-1$ satellite resonances symmetrically disposed with respect to the true resonance center in the limit of infinite magnetic field strength. The spacing between corresponding satellites is constant, independent of the magnetic field strength, and measures the strength of the electric quadrupole interaction.

(b) A central transition whose splitting varies inversely as the resonance frequency. The frequency dependence of this splitting may also be used to determine the quadrupole interaction.

(c) An average shift which is proportional to $1/\nu_R^2$. The infinite field extrapolated value of this shift is the shift of the true resonance center. In addition, the slope of the K_{av} versus $1/\nu_R^2$ plot provides an additional measurement of the quadrupole interaction.

Anisotropic Magnetic Shift Only

Bloembergen has discussed in detail the first-order effects of an anisotropic shift tensor on the resonance line shape in a metallic conductor or paramagnetic substance in the absence of electric quadrupole effects.[10] For the present, we need only consider the results appropriate to the case of an axially symmetric shift tensor. All of the $2I+1$ pure Zeeman levels are shifted by an equal amount in first order, with the result that only a single resonance appears, whose frequency in a single crystal is given by

$$\nu=\nu_0[1+K_{\rm ax}(3\mu^2-1)/(1+K_{\rm iso})]. \quad (10)$$

Here as before, $\mu=\cos\theta$, where now θ is the angle between the z axis of the principal axis system of the shift tensor and the external magnetic field direction. In addition, $K_{\rm iso}$ and $K_{\rm ax}$ are the isotropic and axial components of the shift tensor, respectively. ν_0 represents the pure Zeeman frequency including the isotropic shift contribution, i.e., $\nu_0=\nu_R(1+K_{\rm iso})$. In most cases the isotropic shift is sufficiently small that the distinction between $K_{\rm ax}$ and $K_{\rm ax}/(1+K_{\rm iso})$ is not needed, but in the following we shall employ the notation $a=K_{\rm ax}/(1+K_{\rm iso})$. The angle-dependent factor is seen to be identical with that which occurs in the first-order quadrupole shift of the satellite resonances.

In a polycrystalline sample, the intensity maximum occurs at $\theta=90°$ and the frequency at this point will be

$$\nu^{\rm II}=\nu_0(1-a). \quad (11)$$

Besides this single maximum in the resonance shape, there now also appears a discontinuous step corresponding to $\mu=1$ ($\theta=0°$ or $\theta=180°$).

$$\nu^{\rm I}=\nu_0(1+2a). \quad (12)$$

The notation $\nu^{\rm I}$ and $\nu^{\rm II}$ corresponds to that used in the quadrupolar case, in that $\nu^{\rm I}$ is the high-frequency side of the resonance when $K_{\rm iso}$ and $K_{\rm ax}$ are both positive. Because the resonance intensity depends inversely on the coefficient of the $(3\mu^2-1)$ factor,[9] which is relatively small in the anisotropic shift case, this step is usually observable. Steps also occur in the first-order quadrupole pattern [Eq. (2)], but because then the coefficient of $(3\mu^2-1)$ is so large, the height of the steps is very small, and these are not readily detectable.

Neglecting the Van Vleck dipolar linewidth,[11] the width of the resonance peak due to the anisotropic shift is given by the spacing between the intensity maximum at $\mu=0$ and the step at $\mu=1$,

$$\Delta\nu_{\rm an}=\nu^{\rm I}-\nu^{\rm II}=3a\nu_0=3K_{\rm ax}\nu_R. \quad (13)$$

The intensity maximum at $\mu=0$ lies on the low-frequency side of the resonance if $K_{\rm ax}$ is positive and on the high-frequency side if $K_{\rm ax}$ is negative. Similarly, the step at $\mu=1$ lies on the high-frequency side of the resonance if $K_{\rm ax}$ is positive and on the low-frequency side if $K_{\rm ax}$ is negative. The isotropic and anisotropic shift parameters can be determined by measuring the shift of either $\nu^{\rm I}$ or $\nu^{\rm II}$ and the width $\Delta\nu_{\rm an}$.

Summarizing, the line shape of an NMR line in the case of anisotropic magnetic shift effects only is characterized by

(a) A width which is directly proportional to the resonance frequency or field.

(b) An asymmetric appearance which provides an indication of the sign of the axial component of the shift tensor. For the actual appearance of the theoretical shapes, see Ref. 10.

Combined Nuclear Quadrupole and Anisotropic Shift Effects

Neglecting nuclear dipolar and exchange interactions of the Van Vleck type,[11] the Hamiltonian for N nuclear spins and n conduction electrons in an external magnetic field H_0 in the z direction is written[12]:

$$H=H_0^{(e)}+\sum_{i=1}^{n}\beta H_0(L_z^{(i)}+2S_z^{(i)})+H_0^{(n)}+\sum_{j=1}^{N}g\mu_0H_0I_z^{(j)}+\sum_{i=1}^{n}\sum_{j=1}^{N}H'^{(ij)}. \quad (14)$$

Here, $H_0^{(e)}$ represents the Hamiltonian for the conduction electrons in the field of the ion cores. $H_0^{(n)}$ represents the Hamiltonian for the ion cores. The two terms involving H_0 are the Zeeman energies of the conduction electrons and the nuclei. The term $\sum_{ij}H'^{(ij)}$ describes the noncoulomb interaction of the n conduction electrons with the N nuclei. This latter will be approximated by including only the magnetic dipole and electric quadrupole parts of the interaction, that is, by

$$H'^{(ij)}=\frac{2g\mu_0\beta\mathbf{I}^{(j)}\cdot\mathbf{L}^{(i)}}{hr_{ij}^3}-2g\mu_0\beta\left[\frac{\mathbf{S}^{(i)}\cdot\mathbf{I}^{(j)}}{r_{ij}^3}-\frac{3(\mathbf{S}^{(i)}\cdot\mathbf{r}_{ij})(\mathbf{I}^{(j)}\cdot\mathbf{r}_{ij})}{r_{ij}^5}\right]+\frac{16\pi}{3}g\mu_0\beta\mathbf{S}^{(i)}\cdot\mathbf{I}^{(j)}\delta(\mathbf{r}_{ij})+\sum_{q=-2}^{2}(-1)^qQ_q(\nabla E)_{-q}. \quad (15)$$

The electric quadrupole moment operators Q_q and electric field gradient components $(\nabla E)_q$ are defined by Pound.[8]

In Appendix A it is shown that the second-order contribution of the anisotropic shift portion of $H'^{(ij)}$ is negligibly small, and that the second-order contribu-

[10] N. Bloembergen and T. J. Rowland, Acta Met. **1**, 731 (1953).
[11] J. H. Van Vleck, Phys. Rev. **74**, 1168 (1948).
[12] F. J. Milford, Am. J. Phys. **28**, 521 (1960).

tion resulting from interference terms between the anisotropic shift and quadrupole interactions vanishes identically. With this result, the nuclear Zeeman levels are obtained by adding together the expressions for the anisotropic shift (first order) and for the nuclear quadrupole interaction (second order). The transition frequencies in which we are interested can be obtained in a similar manner by adding together the expressions for the separate interactions.

In the large majority of actual examples encountered to date, the resonant nuclei occupy sites of axial symmetry, so that the electric field gradient tensor is axially symmetric; that is, it can be characterized by a single parameter $q=\partial^2V/\partial z^2$. We shall suppose that the magnetic shift tensor is also axially symmetric, and that the major axes of the two tensors are coincident. This is sufficiently general for understanding most of the examples at hand.

The zeroth order, or pure Zeeman, frequency of this system is just the resonance frequency in the metal or paramagnetic solid,

$$\nu_0=\nu_R(1+K_{\rm iso}). \tag{16}$$

As is shown by (1) and (10) for the case of a single crystal, the first-order quadrupolar and anisotropic shift corrections have the same dependence upon the angle θ between the external magnetic field H_0 and the z axis of the principal axis system of the relevant tensor. Under the assumption that these axes are coincident, we find for the satellite frequencies in first order:

$$\nu(m\rightarrow m-1)=\nu_0\{1+(3\mu^2-1)\times[a+\tfrac{1}{2}(\nu_Q/\nu_0)(m-\tfrac{1}{2})]\}. \tag{17}$$
$$m\neq\tfrac{1}{2}$$

For a polycrystalline sample, the principal maximum intensity for the satellites again occurs when $\mu=0$, so that corresponding to (2), resonance peaks appear at

$$\nu(m\leftrightarrow m-1)=\nu_0\{1-[a+\tfrac{1}{2}(\nu_Q/\nu_0)(m-\tfrac{1}{2})]\}. \tag{18}$$
$$m\neq\tfrac{1}{2}$$

Additional peaks will arise for certain combinations of the values of the various parameters, but these are only significant in the case that both ν_Q and I are large.

Thus, in first order, the effect of the anisotropic shift is to displace all of the satellites by the amount $-a\nu_0$. In a sufficiently strong magnetic field that the second-order quadrupole shifts of the satellites are negligible, we may expect to find their positions determined by (18). The difference between corresponding satellites is seen still to be constant and to be independent of $K_{\rm ax}$.

The satellite resonances in a polycrystalline sample will be correctly described to second order by adding to (18) the second-order terms from (2). Thus, we now have

$$\nu(m\leftrightarrow m-1)=\nu_0\{1-[a+\tfrac{1}{2}(\nu_Q/\nu_0)(m-\tfrac{1}{2})]-\tfrac{1}{16}(\nu_Q/\nu_0)^2[3m(m-1)-I(I+1)+\tfrac{3}{2}]\}. \tag{19}$$
$$m\neq\tfrac{1}{2}$$

for the satellite frequencies. The result mentioned above that the spacing between corresponding satellites is independent of $K_{\rm ax}$ still applies, and in addition, as in the case of quadrupole effects only, the spacing between corresponding satellites is independent of $(\nu_Q/\nu_0)^2$. In other words, the relationship (3) still holds exactly.

More interesting now is the behavior of the shape of the central transition. In a single crystal sample, the frequency of the central transition is given by combining (1) and (10) and setting $m=\frac{1}{2}$:

$$\nu(\tfrac{1}{2}\leftrightarrow-\tfrac{1}{2})=\nu_0\{1+(\nu_Q^2/16\nu_0^2)[I(I+1)-\tfrac{3}{4}]\times(1-\mu^2)(1-9\mu^2)+a(3\mu^2-1)\}. \tag{20}$$

To compute the line shape appropriate to a polycrystalline sample, we have, following Cohen and Reif,[9]

$$P(\nu-\nu_0)d(\nu-\nu_0)=P(\theta)d(\theta)=\tfrac{1}{2}\sin\theta\,d\theta=\tfrac{1}{2}d\mu$$

so that $P(\nu-\nu_0)=\frac{1}{2}|d\nu/d\mu|^{-1}$, $-1\leq\mu\leq1$. Now, from (20),

$$d(\nu-\nu_0)/d\mu=(\nu_Q^2/4\nu_0)\mu\{[I(I+1)-\tfrac{3}{4}]\times(9\mu^2-5)+24\nu_0^2a/\nu_Q^2\}. \tag{21}$$

Again, as in the case of quadrupole effects alone, (4) and (5), this shape function possesses two singularities. These now occur at $\mu=0$ and at

$$\mu=\mu'=\pm\left\{\frac{5}{9}-\frac{8a\nu_0^2}{3\nu_Q^2[I(I+1)-\frac{3}{4}]}\right\}^{1/2}.$$

The μ' singularities are not distinguishable since $\nu-\nu_0$ depends only on μ^2. In addition, a discontinuity or step in the intensity occurs at $\mu=1$, as in the pure quadrupole case. The behavior of the singularities and of the step as a function of the resonance frequency is seen to depend on the sign of $K_{\rm ax}$ as well as on the relative magnitudes of $K_{\rm ax}\nu_0$ and $(\nu_Q)^2/\nu_0$.

Because $0\leq\mu^2\leq1$, the singularity at μ' must satisfy the condition $0\leq(5/9-a\nu_0^2/6b)\leq1$. This means that the range of resonance frequencies within which this singularity will appear is determined by

$$-8b/3a\geq\nu_0^2\geq0 \qquad \text{for } a<0, \tag{22a}$$

$$0\leq\nu_0^2\leq10b/3a \quad \text{for } a>0. \tag{22b}$$

By contrast, the singularity at $\mu=0$ and the step at $\mu=1$ hold for all resonance frequencies. Here, we have introduced the convenient definition, $b=\nu_Q^2[I(I+1)-\frac{3}{4}]/16$. The resonance frequencies corresponding to the two singularities and the step are now seen to be as follows:

$$\nu_H=\nu(\mu=0)=\nu_0+b/\nu_0-a\nu_0, \tag{23a}$$

$$\nu_L=\nu(\mu=\mu')=\nu_0-16b/9\nu_0+\tfrac{2}{3}a\nu_0-a^2\nu_0^3/4b, \tag{23b}$$

$$\nu_S=\nu(\mu=1)=\nu_0+2a\nu_0. \tag{23c}$$

In Fig. 1 we show the behavior of the line shape function $P(\nu-\nu_0)$ as the relative strength of the quadrupole and anisotropic shift interactions is varied from essen-

tially pure quadrupolar to essentially pure anisotropic shift character. The relative strength is represented by the dimensionless parameter $r=a\nu_0^2/b$, and the abscissa is plotted in units of b/ν_0. Figure 1(a) shows the behavior in the case of positive anisotropy and Fig. 1(b) in the case of negative anisotropy. Qualitatively, these two cases differ in the important aspect that for positive K_{ax}, the step moves outside of the two singularities, passing the high frequency ($\mu=0$) singularity at the frequency $\nu_0^2=b/3a$. By contrast, in the case of negative K_{ax}, the step moves toward lower frequencies, remaining between the singularities and merging with the low frequency ($\mu=\mu'$) singularity at $\nu_0^2=8b/3a$. In both cases, the line shape changes gradually from that characteristic of the quadrupole broadened transition to that characteristic of anisotropic shift broadening as a function of the resonance frequency for fixed values of the parameters K_{ax} and ν_Q.

The shift of the resonance can still be determined in the manner described by (9) for the quadrupole effects only case. Only now, the midpoint of the two singularities in the line shape is obtained from the expressions for ν_H and ν_L,

$$\tfrac{1}{2}(\nu_H+\nu_L)=\nu_0-a\nu_0/6-7b/18\nu_0-a^2\nu_0^3/8b\,, \quad (24)$$

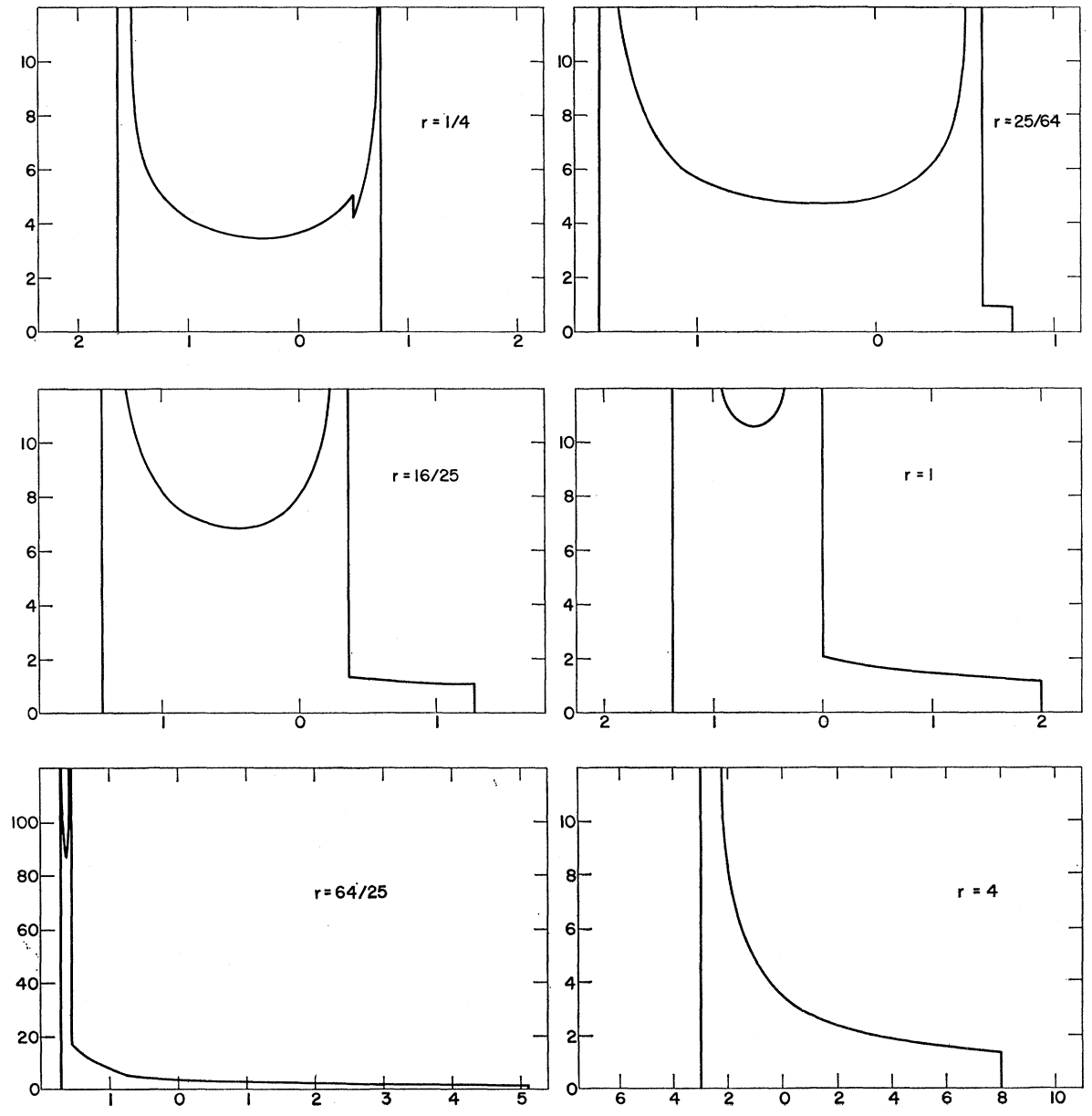

(a)

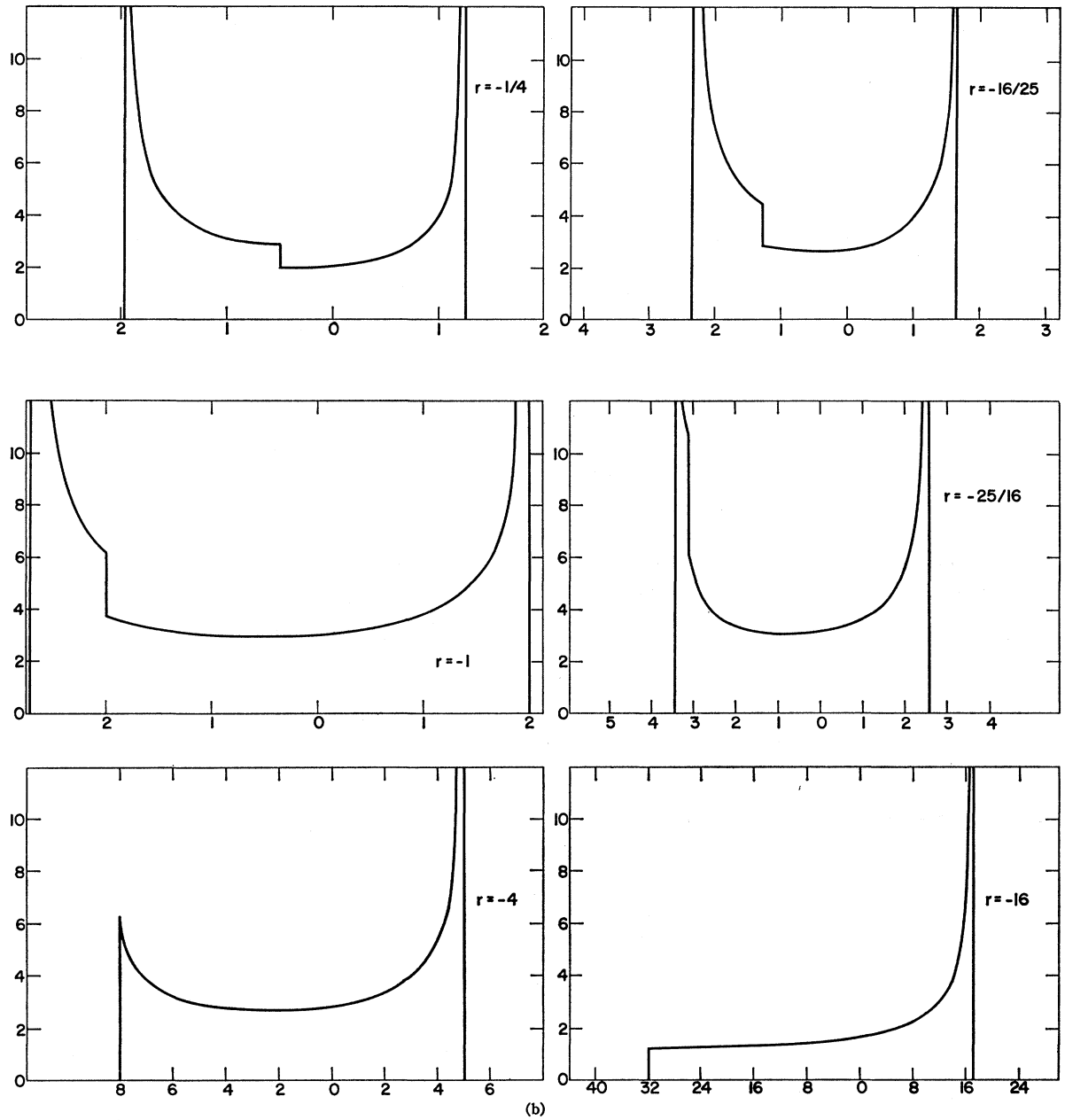

FIG. 1. The line shape function $P(\nu-\nu_0)$ for the case of combined quadrupole and anisotropic shift interactions. The parameter $r=a\nu_0^2/b$ measures the relative strength of the two interactions, and the examples range from essentially pure quadrupole character at the upper left to almost pure anisotropic shift character at the lower right. The abscissa, $(\nu-\nu_0)\nu_0$, is plotted in units of b/ν_0. (a) Positive anisotropic shift, and (b) negative anisotropic shift.

and the average shift is given by

$$K_{\rm av}=\frac{\nu_0-\nu_R}{\nu_R}-\frac{a}{6}-\frac{7b}{18\nu_R^2}-\frac{a^2\nu_R^2}{8b}. \tag{25}$$

Here, as in (9), we have taken $\nu_0=\nu_R$ in all terms except the leading one. Equation (25) shows that the infinite frequency extrapolated value of the average shift now includes a contribution $-K_{\rm ax}/6(1+K_{\rm iso})$ from the anisotropy of the shift, but that the slope of the $K_{\rm av}$ versus ν_R^{-2} plot is determined by the quadrupole interaction exactly as before, provided that the term in ν_R^2 is negligible. In some cases,[2] it is more convenient to measure the separate shifts of the two halves of the split central transition, K_H and K_L, defined by

$$K_H=(\nu_H-\nu_R)/\nu_R=K_{\rm iso}-a+b/\nu_R^2, \tag{26}$$

$$K_L=(\nu_R-\nu_L)/\nu_R=-K_{\rm iso}-2a/3+16b/9\nu_R^2+a^2\nu_R^2/4b, \tag{27}$$

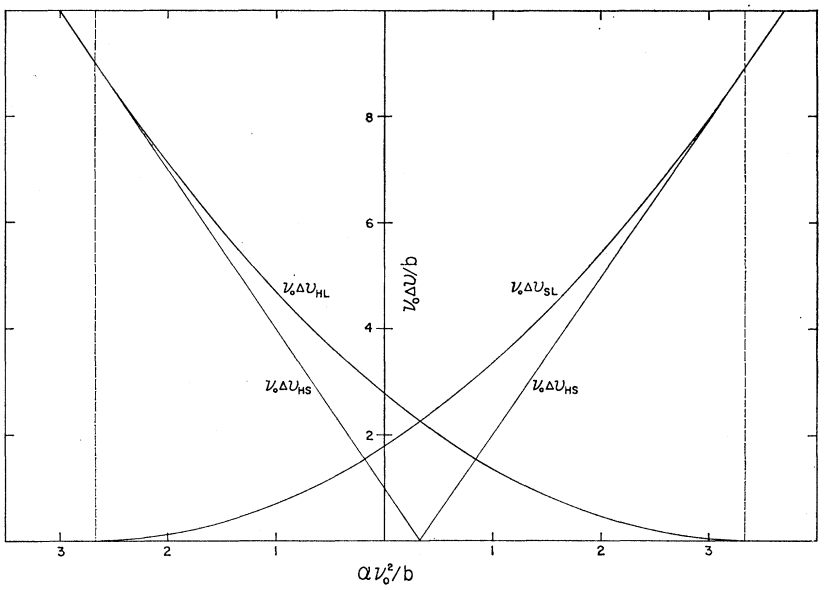

FIG. 2. Behavior of the central transition splittings, $\Delta\nu_{HS}$, $\Delta\nu_{HL}$, and $\Delta\nu_{SL}$ for the case of combined quadrupole and anisotropic shift interactions. The abscissa is plotted in units of the parameter $r=a\nu_0^2/b$ which measures the relative strength of the two interactions, and the ordinate is the product $\nu_0\Delta\nu/b$.

respectively. The infinite frequency extrapolated intercepts of these plots provide two equations in the two unknowns K_{iso} and K_{ax}, and the slopes of the lines again give the value of the quadrupole coupling.

Finally, we consider the various "widths" or splittings of the central transition, which are given by

$$\Delta\nu_{HS}=\nu_H-\nu_S=b/\nu_0-3a\nu_0, \quad (\nu_0^2<b/3a), \tag{28a}$$

$$=3a\nu_0-b/\nu_0, \quad (b/3a<\nu_0^2), \tag{28b}$$

$$\Delta\nu_{HL}=\nu_H-\nu_L=25b/9\nu_0-5a\nu_0/3+a^2\nu_0^3/4b, \tag{28c}$$

$$\Delta\nu_{SL}=\nu_S-\nu_L=16b/9\nu_0+4a\nu_0/3+a^2\nu_0^3/4b, \tag{28d}$$

where the range of validity of (28c) and (28d) is given by (22a) and (22b). The behavior of these splittings is more conveniently represented by the behavior of the product $\nu_0\Delta\nu/b$:

$$\nu_0\Delta\nu_{HS}/b=1-3r, \quad (r<1/3) \tag{29a}$$

$$=3r-1, \quad (r>1/3) \tag{29b}$$

$$\left.\begin{aligned}\nu_0\Delta\nu_{HL}/b&=25/9-5r/3+r^2/4,\\ &\qquad(-8/3\leqslant r\leqslant 0 \text{ for } r<0)\\ \nu_0\Delta\nu_{SL}/b&=16/9+4r/3+r^2/4,\\ &\qquad(0\leqslant r\leqslant 10/3 \text{ for } r>0).\end{aligned}\right\} \tag{29c}$$

Here we have used the variable $r=a\nu_0^2/b$. These products are depicted as functions of r in Fig. 2. Negative values of r correspond to negative K_{ax} and positive values to positive K_{ax}. The range of frequencies within which the splittings $\Delta\nu_{HL}$ and $\Delta\nu_{SL}$ are valid is readily seen in this representation.

To summarize, when both nuclear quadrupole and anisotropic shift effects are present, the nuclear magnetic resonance will be characterized by:

(a) A set of $2I-1$ satellite resonances asymmetrically disposed with respect to the true resonance center in the limit of infinite magnetic field strength. Provided that third and higher order perturbation contributions are negligible, the spacing between corresponding satellites is constant independent of the magnetic field strength and of the anisotropic shift parameter, and is a measure of the strength of the electric quadrupole interaction.

(b) A central transition whose splitting is a function of both the quadrupole and anisotropic shift interactions, and tending in general to vary inversely with resonance frequency at low frequencies and directly at high frequencies.

(c) An average shift which is mainly proportional to ν_R^{-2}. The infinite field extrapolated value of this shift now contains a contribution from the anisotropy of the shift tensor. Alternatively, the shifts of the separate halves of the central transition provide two infinite field intercepts from which the isotropic and axial components of the shift tensor may be determined. The slope of any of the K versus ν_R^{-2} plots provides an additional measurement of the quadrupole interaction.

Numerical Examples

To illustrate the type of behavior to be expected for the splitting of the central transition and for the Knight shift (or paramagnetic shift) of the resonance center, we show here in graphical form some calculated examples based on a quadrupole coupling such that $b=0.18$ $(\text{Mc/sec})^2$ and an isotropic shift of $+0.80\%$. These values are representative of those which have been observed for the Al^{27} resonance in the case of the rare earth–aluminum Laves phase compounds.[4,5] Various combinations of the anisotropic shift parameter a and the intrinsic or dipolar linewidth σ have been taken with these values of b and K_{iso}, and the examples are given only for the splitting $\Delta\nu_{HL}$ which is the one that is usually observed.

Figures 3(a) and 3(b) illustrate the behavior of $\Delta\nu_{HL}$ as a function of ν_0^{-1} as given by (28c). Figure 3(a) shows the case for positive anisotropy, and Fig. 3(b) that for negative anisotropy. Negative anisotropy causes $\Delta\nu_{HL}$ to curve toward higher values at the high-frequency end of the range, whereas a positive anisotropy causes $\Delta\nu_{HL}$ to curve downward at the high-frequency end. The effect of the intrinsic line width σ is simply to displace the entire curve toward larger values.

Figures 4(a) and 4(b) show the behavior of the product $\nu_0\Delta\nu_{HL}$ given by (29c) when a constant linewidth term σ is added. Figure 4(a) emphasizes the behavior of this product in the vicinity of the ordinate intercept $25b/9$, where the effect of σ is to cause a downward curvature of $\nu_0\Delta\nu_{HL}$. Figure 4(b) shows the behavior of $\nu_0\Delta\nu_{HL}$ over a wider range for some of the larger values of a. In this case, the contribution from the term in $r^2=(a\nu_0^2/b^2)$ in (29c) causes an upward curvature at high frequencies.

Figure 5 illustrates the type of behavior that may be expected for the average shift of the resonance as given by (25) for combined quadrupole and anisotropic shift effects. For relatively small values of the anisotropy, the intercept at infinite frequency is altered by the term $-a/6$, but larger values of a have the effect of introducing a downward curvature of K_{av} at high frequencies. This downward curving effect is independent of the sign of a, since it depends only on the a^2 term in (25).

EXPERIMENTAL ILLUSTRATION

Inasmuch as a number of examples of the application of these ideas to the analysis of the spectra resulting from polycrystalline specimens of metals, in particular, have already appeared,[1–3] we include here for illustrative purposes the example of the spectrum of Al^{27} in polycrystalline $PrAl_2$, an intermetallic conductor.[4,5] Due to the presence of both temperature-dependent and temperature-independent contributions to the Knight shift parameters in this case, the extent of interplay between the anisotropic shift and quadrupole interactions is also temperature-dependent, providing in one substance an interesting range of values of the relative strength parameter r [Eq. (29)].

Direct measurement of the satellite spacings (19) of the Al^{27} resonance spectrum at room temperature at three different frequencies gives for the quadrupole coupling, $e^2qQ/h=4.56\pm0.12$ Mc/sec. This means that $\nu_Q=0.684$ Mc/sec, which is relatively small compared to the typical experimental Zeeman frequencies in the range 4–16 Mc/sec. Second-order perturbation theory treatment should still be appropriate.

The presence of anisotropy in the Knight shift is revealed by the splitting $\Delta\nu_{HL}$ of the central transition in the manner shown in Fig. 3(b). The experimental results for room-temperature and liquid-nitrogen temperature are shown in Fig. 6. At both temperatures the $\Delta\nu_{HL}$ plot curves upward at the high frequency end,

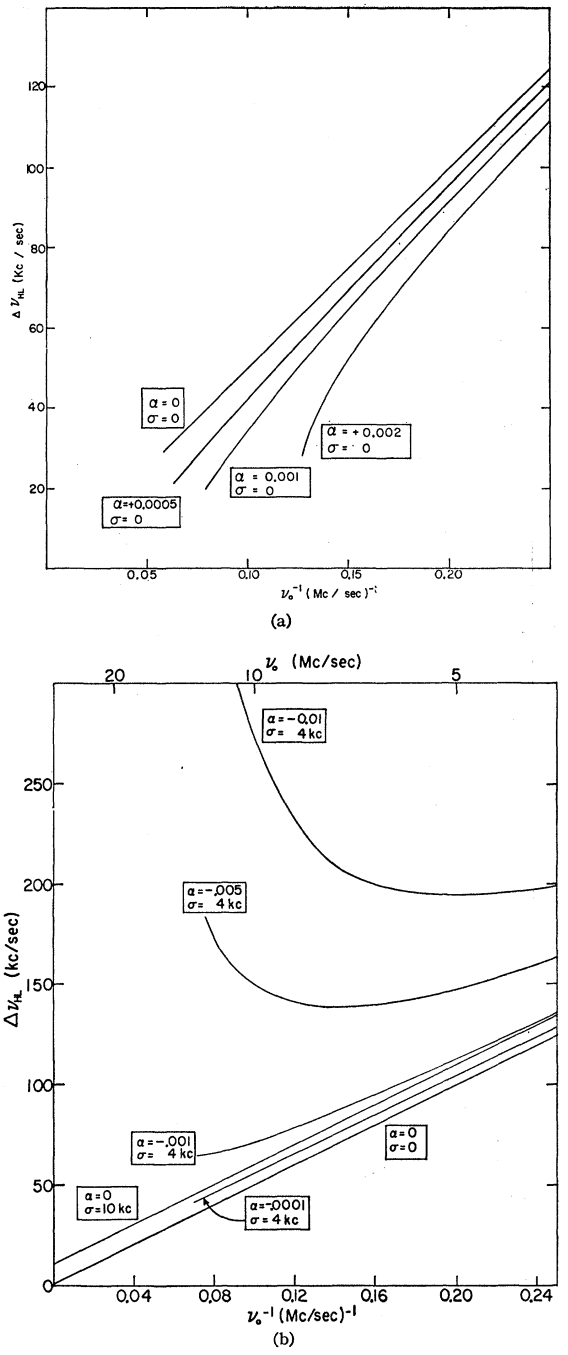

FIG. 3. Splitting of the central transition, $\Delta\nu_{HL}$, as a function of ν_0^{-1} for the case of combined quadrupole and anisotropic shift effects. The quadrupole coupling constant is such that $b=0.18$ (Mc/sec)^2. (a) Positive anisotropic shift values, and (b) negative anisotropic shift values.

indicating that the anisotropy in the shift is negative [Fig. 3(b)]. The degree of curvature is clearly greater at 77°K than at room temperature, showing at once that the shift anisotropy is temperature-dependent.

The solid lines in Fig. 6 are least-squares fittings of the

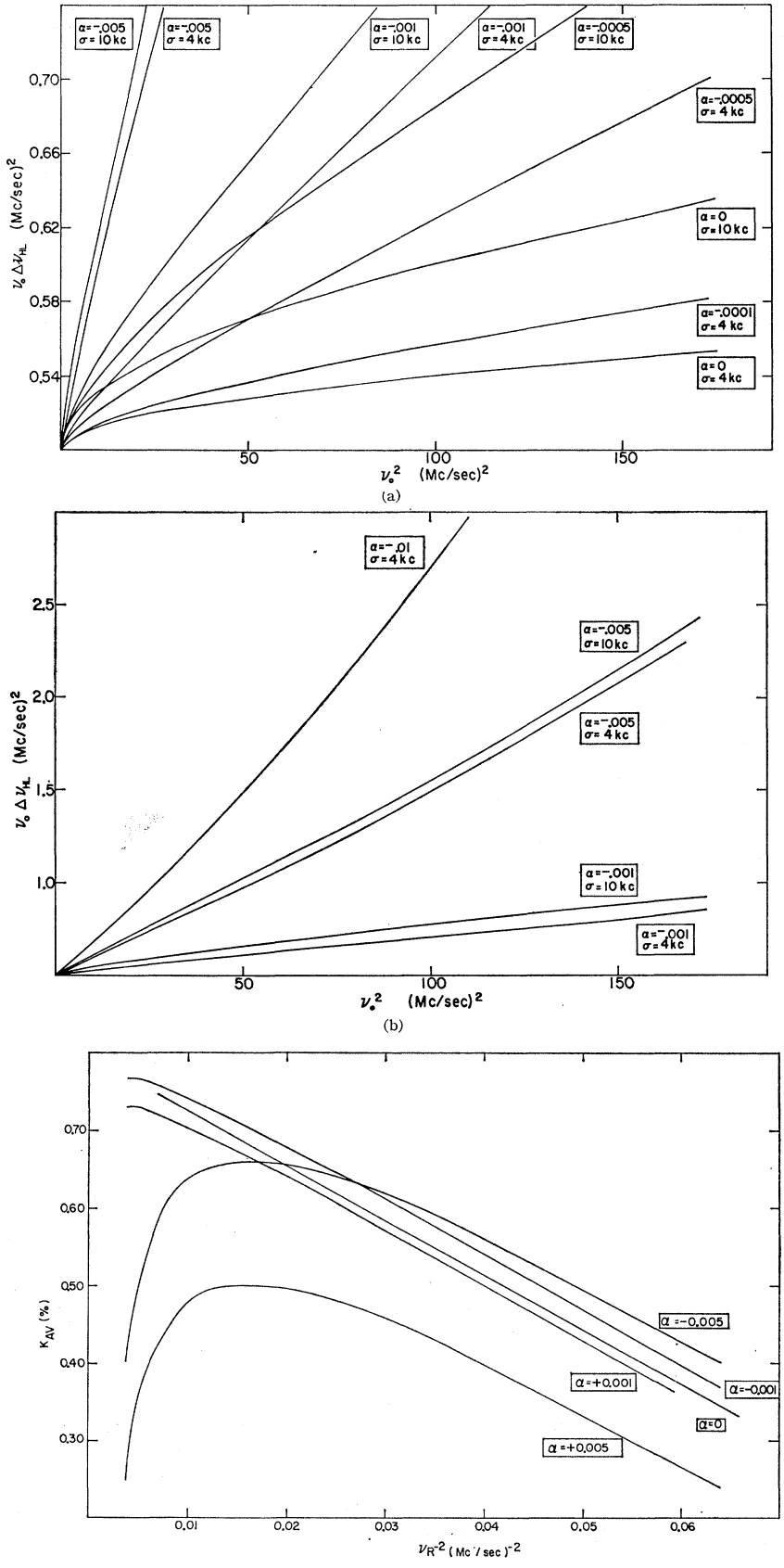

FIG. 4. Behavior of the frequency-splitting product $\nu_0\Delta\nu_{HL}$ as a function of ν_0^2 for the case of combined quadrupole and anisotropic shift effects, and including the effect of a constant linewidth contribution σ. The quadrupole coupling constant is such that $b=0.18$ (Mc/sec)^2. (a) Behavior in the vicinity of the intercept $25\ b/9$ in the case of relatively small values of a, and (b) behavior for relatively large values of a.

FIG. 5. Dependence of the average shift K_{av} on ν_0^{-2} for the case of combined quadrupole and anisotropic shift effects. The quadrupole coupling is such that $b=0.18$ (Mc/sec)^2, and an isotropic shift of $+0.80\%$ has been assumed.

TABLE I. Quadrupole coupling e^2qQ/h, anisotropic Knight shift parameter a, and dipolar linewidth σ, of the Al^{27} nuclear magnetic resonance in polycrystalline $PrAl_2$ based on a least-squares analysis of the splitting of the central transition of the resonance (Fig. 6).

Temp (°K)	e^2qQ/h (Mc/sec)	a (%)	σ (kc/sec)
300	4.50	−0.055	15.1
77	4.69	−0.22	15.0

data points to the equation

$$\Delta\nu_{HL}=25b/9\nu_0-5a\nu_0/3+\tfrac{1}{2}\sigma, \qquad (30)$$

which is (28c) neglecting the term in ν_0^3 (because a is not very large) and including a finite dipolar linewidth contribution $\frac{1}{2}\sigma$. The equations of these lines are found to be (in Mc/sec)

at 300°K: $\Delta\nu_{HL}=0.633\nu_0^{-1}+0.000914\nu_0+0.00754$,

at 77°K: $\Delta\nu_{HL}=0.688\nu_0^{-1}+0.00366\nu_0+0.00749$.

The quadrupole and anisotropy parameters, e^2qQ/h and a, and the dipolar linewidth σ, determined in this fashion, are listed in Table I.

The relative strength parameter r [Eq. (29)] ranges at 300°K from −0.039 at 4 Mc/sec to −0.62 at 16 Mc/sec, and at 77°K from −0.142 at 4 Mc/sec to −2.27 at 16 Mc/sec. This last value approaches the limiting value of −8/3 of (28c), and the contribution $a^2\nu_0^3/4b$ of the cross term in (28c) is then 0.020 Mc/sec. This should be compared with the total line splitting $\Delta\nu_{HL}$ of 0.105 Mc/sec at this temperature and resonance frequency (Fig. 6).

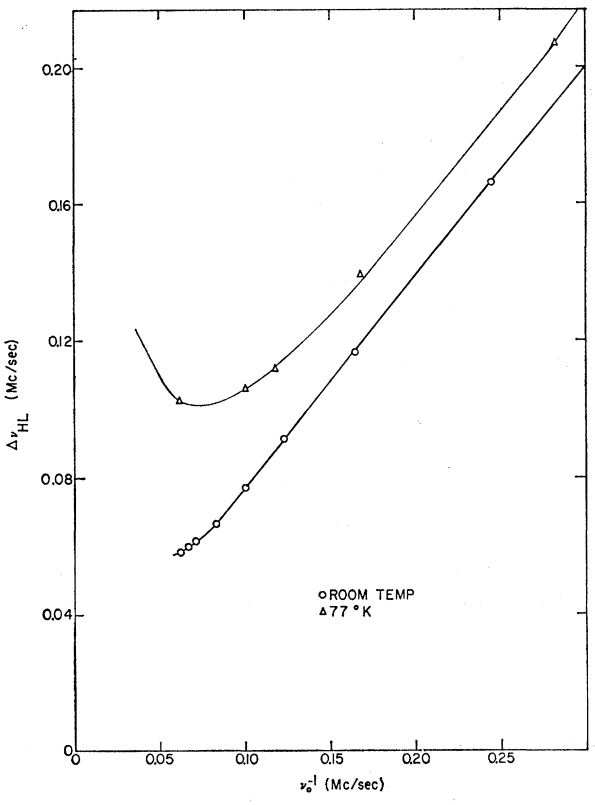

FIG. 6. Splitting of the central transition $\Delta\nu_{HL}$ of the Al^{27} resonance in $PrAl_2$ as a function of ν_0^{-1}. The solid curves are least-squares fittings to Eq. (30) of the text.

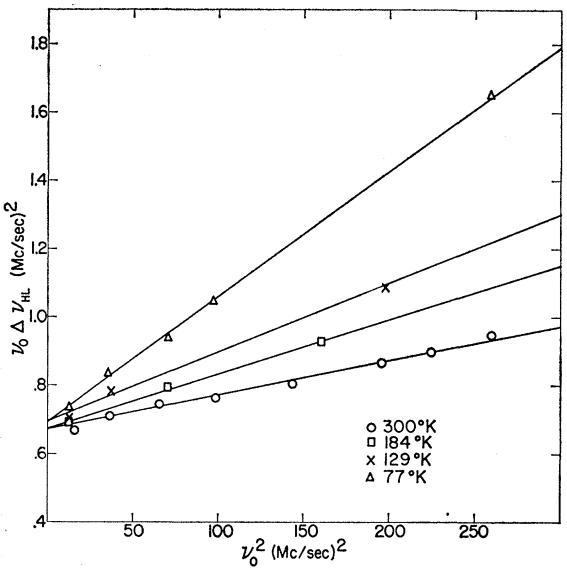

FIG. 7. The product $\nu_0\Delta\nu_{HL}$ for the central transition of the Al^{27} resonance in $PrAl_2$ as a function of ν_0^2. The solid lines are least-squares fittings to $\nu_0\Delta\nu_{HL}=25b/9-5a\nu_0^2/3$.

The central transition splitting measurements may also be handled in the manner of (29) by plotting the product $\nu_0\Delta\nu_{HL}$ as a function of ν_0^2. This is useful when the static dipolar width of the resonance is small, as in the present case. The experimental data for this example are shown in Fig. 7.

Inasmuch as the quadrupole coupling is not large compared to the nuclear Zeeman frequencies employed, measurement of the quantity K_{av} [Eq. (25)], provides a reliable determination of the Knight shift of the resonance. Figure 8 shows the results of room-temperature measurements of K_{av} at eight frequencies in the range 4–16 Mc/sec. The data are shown plotted both as a function of ν_0^{-2} and as a function of ν_0^{-1} to illustrate that the approximation that $K_{av}\sim\nu_0^{-1}$ is not a good one, and cannot be reliably extrapolated to the true infinite field value of the shift. The quadrupole coupling determined from the slope of the K_{av} versus ν_0^{-2} line in Fig. 8 is $e^2qQ/h=4.59$ Mc/sec, in agreement with the values determined from the satellite spacing and from the splitting of the central transition.

The infinite frequency intercept of the K_{av} versus ν_0^{-2} line is +0.526%. Using the value of a from Table I, we have from (25) at infinite frequency:

$$K_{iso}=K_{av}+\tfrac{1}{6}a \qquad (31)$$

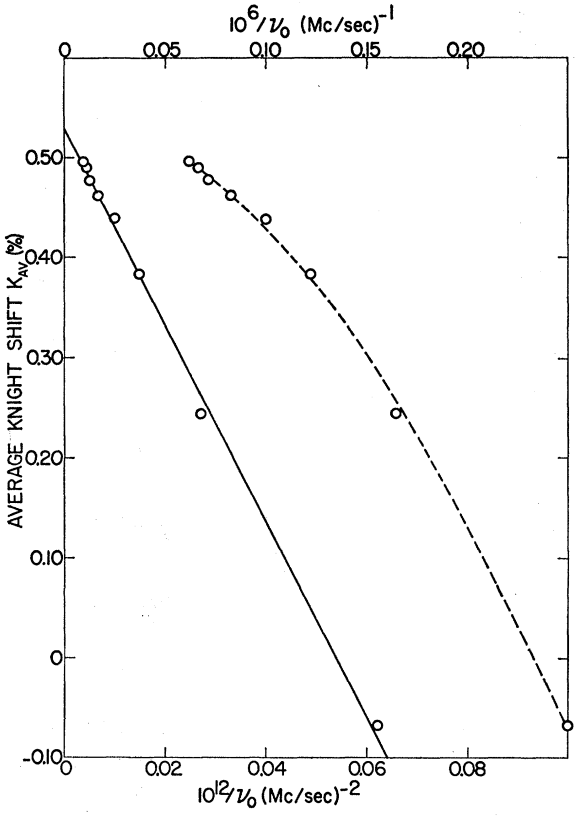

FIG. 8. Average Al^{27} Knight shift K_{av} in $PrAl_2$ at room temperature as a function of ν_0^{-2} (bottom scale and solid line) and of ν_0^{-1} (top scale and broken line).

so that in the present case, $K_{iso}=+0.517\%$. In the same manner, the value of K_{iso} is obtained at other temperatures to complete the characterization of the experimental data in terms of K_{iso}, a, and e^2qQ/h.

ACKNOWLEDGMENTS

The authors express their indebtedness to Dr. F. J. Milford for making available some of his unpublished work on the hyperfine interaction Hamiltonian, and for a number of valuable discussions. The interest and comments of S. L. Segel and D. R. Torgeson have also been appreciated.

APPENDIX A

We shall consider the interplay of the Knight shift with the quadrupole terms.[13] The S_zI_z portion of the contact term in (15) simply contributes a small additional field at the nucleus which results in an additional Zeeman splitting and shift of all the resonances by the same amount. This is the usual Knight shift. The remaining terms in the contact interaction are of the form S_+I_- or S_-I_+, neither of which has diagonal matrix elements. In second-order perturbation theory each would contribute to a term involving an energy denominator of the order βH_0 due to the flip of electron spins. These terms are small to order $g\mu/\beta\sim10^{-3}$ compared to either diagonal Knight shift terms or second-order quadrupole terms and thus may be neglected. The same argument enables us to eliminate a number of terms in the balance of (15), and to write finally, $H'^{(ij)}=H'_{KA}+H'_Q$, with

$$H'_{KA}=-2g\mu_0\beta\sum_k\left\{\frac{S_{zk}I_{zj}}{r_{jk}^3}-\frac{3(S_{zk}z_{jk})(\mathbf{I}_k\cdot\mathbf{r}_{jk})}{r_{jk}^5}\right\} \quad \text{(A1)}$$

which will be referred to as the anisotropic Knight shift interaction. H'_Q is the quadrupole interaction and is the last term of (15). The operator H'_{KA} is diagonal in the electron spins; it can be further broken down into a part which is diagonal in the nuclear spin and a part which is not:

$$H'_{KA}=H'_{KAd}+H'_{KA0}. \quad \text{(A2)}$$

The individual operators are

$$\begin{aligned}H'_{KAd}&=-2g\mu_0\beta I_{zj}\sum_{k=1}^{n}S_{zk}(1-3\cos\theta_{jk})/r_{jk}^3,\\ H'_{KA0}&=6g\mu_0\beta\sum_{k=1}^{n}S_{zk}[\cos\theta_{jk}\\ &\quad\times(I_{jx}\cos\phi_{jk}+I_{jy}\sin\phi_{jk})\sin\theta_{jk}]/r_{jk}^3.\end{aligned} \quad \text{(A3)}$$

The shift in energy of the mth nuclear level will be given by

$$\Delta E_m=(H'_Q+H'_{KAd})_{mm}+\sum_{m'}|(H'_Q+H'_{KA0})_{mm'}|^2/(E_m-E_{m'}). \quad \text{(A5)}$$

Here, the dipole-dipole term has been omitted on the basis of Silver's arguments.[14] The second-order term in ΔE_m can be expanded

$$E_m^{(2)}=\sum_{m'}\{|(H'_Q)_{mm'}|^2+2\,\mathrm{Re}(H'_Q)_{mm'}(H'_{KA0})_{m'm}+|(H'_{KA0})_{mm'}|^2\}(E_m-E_{m'})^{-1}. \quad \text{(A6)}$$

With respect to (A6), the first question to be resolved is that of the relative sizes of the second terms. One basis for accomplishing this is to assume that

$$(H'_Q)_{mm'}\approx\beta,\quad (H'_{KA0})_{mm'}\approx(H'_{KAd})_{mm}\approx\alpha,$$

and that in the cases of interest, $\alpha\approx\beta^2/h\nu_L$. Then,

$$\Delta E_m^{(2)}\approx\frac{\beta^2}{h\nu_L}+\frac{2\beta\alpha}{h\nu_L}+\frac{\alpha^2}{h\nu_L}\approx\frac{\beta^2}{h\nu_L}+\frac{2\beta^3}{(h\nu_L)^2}+\frac{\beta^4}{(h\nu_L)^3}. \quad \text{(A7)}$$

With $\beta/h\nu_L\ll1$, it is clear that the second and third terms give contributions which are small compared to the first. This justifies neglecting these terms if the

[13] F. J. Milford (unpublished).

[14] A. H. Silver, J. Chem. Phys. 32, 959 (1960).

assumption that $(H'_{KA0})_{mm'} \approx (H'_{KAd})_{mm}$ can be verified. It would be equally useful to establish that $(H'_{KA0})_{mm'} < (H'_{KAd})_{mm}$.

To investigate this point we now assume axial symmetry for the electron distribution. Let the coordinates x, y, z be so chosen that the z-axis is the symmetry axis. An arbitrary point is specified by the coordinates r, Θ, Φ. Furthermore, let the axes ξ, η, ζ be such that H_0 is along ζ and makes polar angles θ, ϕ with the x, y, z coordinates. Choose ξ to lie in the x, y plane, making an angle $\phi-\pi/2$ with the x axis.

In terms of these coordinates one may, following Bloembergen and Rowland,[10] write

$$\begin{aligned} H'_{KAd} &= -g\mu_0\beta I_{\zeta j}\sum_k S_{\zeta k}(1-3\cos^2\theta_{jk})/r_{jk}^3 \\ &= -2g\mu_0\beta I_{\zeta j}\sum_k \sum_{l=-2}^{+2}(-1)^l S_{\zeta k} \\ &\quad \times P_2^{\,l}(\cos\Theta)P_2^{\,-l}(\cos\theta)e^{il(\Phi-\phi)}/r_{jk}^3, \end{aligned} \tag{A8}$$

where the z subscript on the spin operators has been changed to ζ in order to agree with the coordinates introduced above. Continuing with the assumption of axial symmetry, one may assume that the electronic wave functions have the form

$$\psi^*\psi = r^2 g(r)[A+(C-A)\cos^2\Theta], \tag{A9}$$

if only s and p states are included. Then, as Bloembergen and Rowland have shown,[10]

$$\begin{aligned} (H'_{KAd})_{mm} &= \left(\frac{16\pi}{15}\right)g\mu_0 H_0 \chi_p \Omega(3\cos^2\theta-1)(C-A) \\ &\quad \times \int_0^\infty r g(r)dr \\ &= Fh\nu_0(3\cos^2\theta-1), \end{aligned} \tag{A10}$$

where the last equality defines F.

For the off-diagonal part H'_{KA0} we have

$$H'_{KA0} = 6g\mu_0\beta\sum_k S_{\zeta k}I_{\xi j}\cos\theta_{jk}\sin\theta_{jk}\cos\phi_{jk}/r_{jk}^3, \tag{A11}$$

plus a similar term involving $I_{\eta j}$. Changing variables to Θ, Φ; θ, ϕ gives

$$\begin{aligned} H'_{KA0} &= 6g\mu_0\beta\sum_k S_{\zeta k}I_{\xi j}r^{-3}\sin\Theta[\cos\Phi\sin\phi-\sin\Phi\cos\phi] \\ &\quad \times[\sin\theta\cos\phi\sin\Theta\cos\Phi \\ &\quad +\sin\theta\sin\phi\sin\Theta\sin\Phi+\cos\theta\cos\Theta]. \end{aligned} \tag{A12}$$

Again taking $\psi^*\psi$ as given by (A9), one finds

$$\begin{aligned} (H'_{KA0})_{mm'} \sim \int & r^{-1}g(r)[A+(C-A)\cos^2\theta] \\ & \times\sin\Theta[\cos\Phi\sin\phi-\sin\Phi\cos\phi] \\ & \times[\sin\theta\cos\phi\sin\Theta\cos\Phi+\sin\theta\sin\phi\sin\Theta\sin\Phi \\ & +\cos\theta\cos\Theta]r^2\sin\Theta dr d\Theta d\Phi. \end{aligned} \tag{A13}$$

It is convenient to do the Φ integration first, and this leads to

$$\begin{aligned} (H'_{KA0})_{mm'} \sim \int & r g(r)dr\int_0^\pi [A+(C-A)\cos^2\theta] \\ & \times[\sin\theta\cos\phi\sin\phi\sin\Theta \\ & -\sin\phi\sin\theta\cos\phi\sin\Theta]\sin^2\Theta d\Theta \\ & =0. \end{aligned} \tag{A14}$$

The same argument applies to the term involving $I_{\eta j}$.

As a consequence of (A14), the second-order energy shift (A6) reduces rigorously to the second-order quadrupole shift alone.